BMC Microbiology

RESEARCH

Open Access

Interactions between *Helcococcus kunzii* and *Staphylococcus aureus*: How a commensal bacterium modulates the virulence and metabolism of a pathogen in a chronic wound in vitro model

Benjamin A. R. N Durand[1], Riham Daher[1], Lucia Grenga[2], Madjid Morsli[1], Jean Armengaud[2], Jean-Philippe Lavigne[1] and Catherine Dunyach-Remy[1*]

Abstract

Background Staphylococcus aureus is the predominant pathogen isolated in diabetic foot infections. Recently, the skin commensal bacterium, Helcococcus kunzii, was found to modulate the virulence of this pathogen in an in vivo model. This study aims to elucidate the molecular mechanisms underlying the interaction between these two bacterial species, using a proteomic approach.

Results Our results reveal that H. kunzii can coexist and proliferate alongside S. aureus in a Chronic Wound Media (CWM), thereby mimicking an in vitro chronic wound environment. We noted that the secreted proteome of H. kunzii induced a transcriptional effect on S. aureus virulence, resulting in a decrease in the expression level of agrA, a gene involved in quorum sensing. The observed effect could be ascribed to specific proteins secreted by H. kunzii including polysaccharide deacetylase, peptidoglycan DD-metalloendopeptidase, glyceraldehyde-3-phosphate dehydrogenase, trypsin-like peptidase, and an extracellular solute-binding protein. These proteins potentially interact with the agr system, influencing S. aureus virulence. Additionally, the virulence of S. aureus was notably affected by modifications in iron-related pathways and components of cell wall architecture in the presence of H. kunzii. Furthermore, the overall metabolism of S. aureus was reduced when cocultured with H. kunzii.

Conclusion Future research will focus on elucidating the role of these excreted factors in modulating virulence.

Keywords Bacterial interactions, Chronic wound, *Helcococcus kunzii*, *Staphylococcus aureus*, In vitro model, Proteomic analysis

*Correspondence:
Catherine Dunyach-Remy
catherine.remy@chu-nimes.fr
[1]Department of Microbiology and Hospital Hygiene, CHU Nîmes, VBIC, INSERM U1047, Univ Montpellier, Nîmes, France
[2]Département Médicaments et Technologies pour la Santé (DMTS), Université Paris-Saclay, CEA, INRAE, Bagnols-sur-Cèze, SPI, France

Background

Chronic wounds pose a significant public health challenge, characterized by prolonged and complex management, with a high risk of recurrence, and associated costs. Complications related to chronic wounds amplify the economic burden and deteriorate patients' quality of life [1]. Among these complications, bacterial infections frequently cause healing delays. Managing these infections remains challenging due to the difficulty in distinguishing between bacterial colonization and wound infections.

Chronic wounds display characteristics of a polymicrobial environment [2], where pathogenic and commensal bacteria form biofilm structures [3]. This biofilm formation contributes to wound healing delays [4]. Interactions between microorganisms play a crucial role in modulating pathogen virulence, aiming to evade the host's immune defenses. This organization fosters bacterial persistence and contributes to the chronicity of the wound. The microbial community composition in chronic wounds exhibits considerable interpersonal variability [5], with no distinct pathogens but rather a combination of associated species that either worsen or improve the wound condition [6, 7]. The intricate network of interactions among species in close contact elicits cooperative or antagonist effects [4]. Understanding this network of microbial crosstalk and cooperation between commensal and pathogenic bacteria is a priority to enhance the management of these challenging wounds.

S. aureus is the main pathogenic bacteria found in chronic wounds [8]. A study observed a coaggregation of *S. aureus* and a commensal Gram-positive cocci isolated from cutaneous microbiota, *Helcococcus kunzii* [9]. We previously studied the virulence phenotypes of these species, both individually and in association, using a *Caenorhabditis elegans* model. While *H. kunzii* strains did not reduce worm survival, confirming their commensalism, their association with *S. aureus* could modulate the virulence potential of the pathogen [10]. This attenuation was linked to the ability of certain *H. kunzii* strains to downregulate the key virulence regulator of *S. aureus*, the *agr* system [10].

The *agr* system is induced during the transition from late exponential growth to the stationary phase, and is sustained throughout the stationary phase, enabling the production of several virulence factors [11]. We recently conducted a genomic comparison study to elucidate potential interaction mechanisms. Two main hypotheses were explored: (i) *H. kunzii* proteins secretion with a direct effect on the *agr* system through ligand antagonistic competition for AgrC and (ii) modulation of bacterial metabolism, specifically targeting iron-related metabolism [12]. Of the five potential candidates identified, three were produced by the *H. kunzii* strain with the in silico capacity to attenuate *S. aureus* virulence [13].

The objective of this study was to identify potential proteins (from intracellular or secreted fractions) produced by *H. kunzii* involved in decreasing *S. aureus* virulence, and to describe the impact of *H. kunzii* on the *S. aureus* virulence regulatory network and global metabolism.

Materials and methods

Strains and media

The strains used were isolated from Grade 3 infected foot ulcers in patients living with diabetes. The NSA739 strain is an *S. aureus* strain belonging to ST8 [14]. H13 is an *H. kunzii* strain known for its potent activity against *S. aureus* virulence [9, 10]. All strains are part of the collection of the Department of Microbiology at Nîmes University Hospital (France). This study was submitted to the Institutional Review Board (IRB) of University Hospital, Nîmes, France which deemed it unnecessary to obtain a patient consent to participate according to national regulation. In fact, the analysis of biological samples was obtained in the context of medical care and was considered as non-interventional research. Moreover, this study only uses bacterial strains and does not involve human specimens or explore clinical data. In this context, the IRB judged that only the non-opposition of the patient during sampling was required according to articles L1221-1.1, L1211-2, and N°DC-2020-4155 of the French Public Health Code. The consent to participate was waived by the IRB of University Hospital, Nîmes.

Cultures of the strains were obtained using Luria Bertani broth Agar (LBA) for isolating *S. aureus* and Trypticase Soy supplemented with 5% sheep blood (TSS, Biomerieux, Marcy l'Etoile, France) agar media for isolating both *S. aureus* and *H. kunzii*. Additionally, we used an in vitro modified Chronic Wound Medium (CWM) [15] that mimics conditions encountered in wounds. This medium initially contained 20% serum, 0.5% blood, and 79.5% Bolton broth. However, it was adapted here with 5% serum, 0.125% blood, and 94.87% Bolton broth to reduce contamination from human-origin proteins for the proteomic analysis.

Mono- and coculture assays

Coculture experiments and their corresponding monocultures were conducted using the modified CWM. 40 mL of NSA739 and H13 precultures were grown for 24 h at 37 °C with shaking at 250 rpm under aerobic or anaerobic conditions, respectively. The cultures were then centrifuged at 4000 rpm for 150 s. Bacterial interactions were monitored during exponential and stationary phases. Cell pellets were resuspended in 6 mL of Bolton base broth (Sigma-Aldrich, Saint-Quentin-Fallavier, France), and the optical density (OD_{600nm}) was adjusted to 0.1 (±0.02) (to evaluate the exponential and early stationary phase, in a 1 to 3 ratio in favor of *H. kunzii*, and 1 (±0.3) to evaluate

the stationary phase. The resulting bacterial suspensions were added on top of a 6 mL layer of solid CWM in 25 cm^3 flasks. Cultures were anaerobically incubated for 24 h at 37 °C under constant agitation at 50 rpm. In parallel, to assess the number of viable bacteria after *H. kunzii* and *S. aureus* cocultures, CFU counts were performed at 0, 6, 16, and 24 h on LBA and TSS agar media. Colonies grown on TSS were differentiated based on their morphology: *H. kunzii* colonies appeared as pinhead translucent grey, while *S. aureus* formed hemolytic, yellowish, and larger ones. In addition, the CFU counts of *S. aureus* were compared between LB and TSS agar medium.

After 24 h, bacterial suspensions were collected in 15 mL tubes and centrifuged for 10 min at 4,000 rpm at +4 °C. The bacterial pellets were washed with 1 mL of PBS 1X (Sigma-Aldrich), centrifuged at 10,000 rpm for 180 s, and then resuspended in 60 µL of LDS 1X (Lithium duodecylsulfate; NuPAGE, ThermoFisher, Waltham, MA, USA) supplemented with 5% β-mercaptoethanol (Sigma-Aldrich) before being stored at -20 °C. To obtain the exoproteome, the culture supernatants were filtered through a 0.22 µm membrane (syringe filter; VWR, Rosny sous Bois, France). Aliquots of 200 µL were then transferred into 2 mL tubes (Sarstedt, Marnay, France). Proteins were precipitated by chloroform-methanol extraction, as previously described [16]. The resulting protein pellet was air-dried before being resuspended in 30 µL of LDS 1X supplemented with 5% β-mercaptoethanol and stored at -20 °C.

Hemolysin test assay

NSA739 and H13 precultures were grown for 24 h and 48 h at 37 °C with shaking at 250 rpm under aerobic or anaerobic conditions, respectively. *S. aureus* and *H. kunzii* were diluted at 1/10,000 and 1/100, respectively. The resulting bacterial suspensions were cultivated together and adjusted to a 1:1 ratio. Cultures were anaerobically incubated for 24 h at 37 °C under constant agitation at 250 rpm. Serial dilutions of the monoculture and coculture suspensions were performed and 100 µL of each culture was plated on TSS agar media for 24 h in anaerobic conditions. Hemolysin colonies were counted and the percentage of hemolysis was calculated and compared between mono and coculture. Colonies grown on TSS were differentiated based on their morphology.

Medium enriched with *H. kunzii* exoproteome (MEHkE) preparation and *agrA* transcriptomic study

To study the role of *H. kunzii* secreted proteome on the *agrA* gene at the transcriptomic level, *S. aureus* was growth in a medium containing this secreted proteome, adapted from [17]. Briefly, a preculture of *H. kunzii* H13, described above, was centrifugated. The supernatant was precipitated in chloroform-methanol and resuspended in LDS 1×(2.2 mL supernatant in 500 µL LDS 1X) to concentrate secreted proteins. This MEHkE solution was stored at -20 °C. Then, 5 mL of modified CWM was inoculated with NSA739 at the OD adjusted to 0.1 or 1 and supplemented with 0.1 mL LDS 1X MEHkE solution. A negative control with LDS 1X alone was performed. Cultures were incubated for 24 h at 37 °C under 250 rpm. After centrifugation (10 min at 4,000 rpm and 4 °C), *S. aureus* pellets were stored at -80 °C before RNA extraction.

Cell pellets from MEHkE exposed *S. aureus* culture and coculture were treated in the same way, following an adapted protocol from [18]. The bacterial fraction was washed once with 1 mL Tris Triton EDTA (TTE) 1X and then extracted according to the RNAeasy Plus kit (Qiagen, Courtaboeuf, France), following the manufacturer's recommendations with two extra-steps. Culture samples were resuspended in 200 µL TTE1X added to 10 µL of a solution of lysozyme (10 µg/mL), lysostaphin (1 mg/mL), and mutanolysin (62.5 µg/mL) (Sigma-Aldrich) and were further incubated for 30 min at 37°C. After the first column wash, a DNAse treatment was performed using 10µL of DNAse (Qiagen) and 70µL of DNAse Buffer (Qiagen). Extracted RNAs were quantified using an ELISA plate reader (ThermoFisher) and further normalized at 50 ng/µL. Reverse transcription was performed using iScript™ Reverse Transcription Supermix for RT-qPCR (BioRad, Marne La Coquette, France). Reverse transcription products were quantified and normalized to 50 ng/µL. Quantitative PCR assay was performed using 2 µL of normalized cDNA (50ng/µL), 1.2 µL of each target primers (10 mM), 2.4 µL LightCycler® RNA Master SYBR Green I kit (Roche Applied Science, Meylan, France) for a total of 10 µL per well in a LightCycler®480 device (Roche Diagnostics, Meylan, France). Primers used were agrA-F (5′- CAA AGA GAA AAC ATG GTT ACC ATT ATT AA-3'), agrA-R (5′- CTC AAG CAC CTC ATA AGG ATT ATC AG-3') [19], gyrB-F (5'- GGT GGC GAC TTT GAT CTA GC-3'), gyrB-R (5'- TTA TAC AAC GGT GGC TGT GC-3') [20]. 35 PCR cycles were programmed with 30s of denaturation, 30s of hybridization at 52 °C and 1 min of elongation. Cycle threshold (*Ct*) values of the different target genes were compared with the *Ct*-values of the house-keeping gene (*gyrB*) [21]. Amplifications were performed in triplicate from three different RNA preparations. The $\Delta\Delta C_t$ were calculated following the equation [22]: $2^{-\Delta\Delta Ct}$ ($\Delta\Delta Ct = (Ct_{gene} - Ct_{gyrB})_{NSA739\ exposed\ to\ H.\ kunzii} - (Ct_{gene} - Ct_{gyrB})_{NSA739\ alone}$).

Whole genome sequencing

The *H. kunzii* and *S. aureus* genomes were sequenced according to the Illumina library preparation protocol using 250 ng of the extracted DNA following the DNA Prep kit library paired-end protocol (Illumina, San Diego,

USA) and sequenced in a 39-h run providing 2×250-bp reads on a Miseq sequencer (Illumina), as previously described [23]. Both genomes were *de novo* assembled using Spades software (version 3.15.4) and annotated using DDBJ Fast Annotation and Submission Tool online platform (https://dfast.ddbj.nig.ac.jp/), then compared by Pangenome analysis using Roary tools (Version 3.13.0).

Proteomic study during the *H. kunzii* and *S. aureus* interaction

Tryptic peptides were obtained and identified from the exoproteome and proteome samples as previously described [13]. Briefly, peptides were identified using an UltiMate 3000 nano-LC system (ThermoFisher Scientific) coupled to a Q Exactive HF mass spectrometer (ThermoFisher Scientific). Peptides were desalted on a reverse-phase PepMap 100 C18 µ-precolumn (5 µm, 100 Å, 300 µm i.d. × 5 mm, ThermoFisher Scientific) before separation on a nanoscale PepMap 100 C18 nano-LC column (3 µm, 100 Å, 75 µm i.d. × 50 cm, ThermoFisher Scientific) using a 90 min gradient (75 min from 4 to 25% solvent B, and 15 min from 25 to 40% of solvent B) at a flow rate of 0.2 µL per min. Solvent A was 0.1% formic acid in water, while solvent B was 80% acetonitrile, 0.1% formic acid in water. The mass spectrometer was operated in Top 20 mode, acquiring full MS from 350 to 1500 m/z, and selecting the 20 most abundant precursor ions for fragmentation, with a 10-s dynamic exclusion window. Ions with charge 2+and 3+were chosen for MS/MS analysis, and secondary ions were isolated within a 2.0-m/z window. Data were interpreted using the Mascot Daemon software version 2.6.0 (Matrix Sciences, Chicago, IL, USA) by searching a database comprising 82,248 polypeptide sequences, representing the annotated genomes of *H. sapiens*, *H. kunzii* H13 strain (NZ_CP048105.1) and *S. aureus* Newman strain (AP009351.1) as detailed in [13]. Newman strain is closely similar to NSA739 exhibiting>99% genome coverage and identity. The coding ratios are closely similar Pangenome comparison yielded that the totality of proteins predicted in the NSA739 genome was found in the Newman strain, justifying the choice of this strain.

Regulator and virulence genes transcriptomic study

Mono and cocultures, RNA extractions, and qRT-PCRs were made with the same protocol described in previous sections. Primers used were hla-F (5'- TCC AGT GCA ATT GGT AGT CA-3'), hla-R (5'- GGC TCT ATG AAA GCA GCA GA -3'), spa-F (5'- TAT GCC TAA CTT AAA TGC TG -3'), spa-R (5'- TTG GAG CTT GAG AGT CAT TA -3'), sarA-F (5'- TGT TTG CTT CAG TGA TTC GT-3'), sarA-R (5' CAG CGA AAA CAA AGA GAA AG -3', sigB-F (5'- TGG CGA AAG AGT CGA AAT CAG C-3'), sigB-R (5'- TCA GCG GTT AGT TCA TCG CTC AC -3') [20].

Statistical and bioinformatic analysis

Comparison of *agrA* expression in *S. aureus* with and without the presence of *H. kunzii* was analyzed using the Student's t-test with GraphPad Prism (v9.2.0) (San Diego, CA, USA). Regarding the proteomic analysis, normalization of spectral counts, their variation, and visualization were carried out using an R script [24–28]. Statistical analysis of proteomic data was performed using Perseus software (v1.6.5.0) [29] allowing for permutated FDR correction; this correction accounted for both fold change and p-values through a nonlinear weighting.

Results

Validation of coculture conditions to proteomic assays

The coculture growth potential of *H. kunzii* and *S. aureus* was evaluated. At an initial OD_{600}=1, the CFU at T0 were, on average, 2.82×10^8 CFU/mL and 3.4×10^8 CFU/mL for *S. aureus* and *H. kunzii*, respectively (n=3). After 24 h of contact time, these counts increased to 1.14 10^9 and 4.23 10^8 CFU/mL, respectively, indicating stability over the duration of the contact time (Fig. 1A). When the initial OD_{600} was set at 0.1, *H. kunzii* began at 1.2 10^7 CFU/mL, and reached 7.6 10^8 CFU/mL after 24 h. In contrast, *S. aureus* started at 2.86 10^7 CFU/mL and reached 1.8 10^9 CFU/mL, suggesting that both species had entered an exponential growth phase (Fig. 1B). By the 24 h mark, the proportions of both species were comparable.

The growth kinetics of the coculture were investigated at an initial OD_{600} of 0.1 (Fig. 1C). Both *S. aureus* and *H. kunzii* started at 1.77 10^7 and 3.9 10^7 CFU/mL, respectively. The exponential phase of *S. aureus* commenced immediately and concluded after 5 h, reaching a stationary phase at 1.9 10^8 CFU/mL. In contrast, *H. kunzii* displayed a different growth profile, with an initial lag phase of 16 h (6 10^7 CFU/mL), followed by an exponential phase that led to its stationary state at 21 h with 1.03 10^8 CFU/mL. At 24 h, both strains were found in equivalent ratios, with 2.46 10^8 and 2.1 10^8 CFU/mL for *S. aureus* and *H. kunzii*, respectively. Interestingly, the *H. kunzii* strain in coculture began active replication when the *S. aureus* strain had already reached its stationary phase. In monoculture, with a starting inoculum at 4.66 10^7 CFU/mL, *H. kunzii*'s lag phase was shorter, resolving after 5 h (6 10^7 CFU/mL), and reaching a stationary phase (4 10^8 CFU/ml) by 16 h. Additionally, the growth kinetics of *S. aureus* remained unchanged, whether cultivated alone or in combination with *H. kunzii* (Figure S1). These results demonstrate that, at 24 h in both mono and coculture conditions, the two species underwent a complete exponential phase and entered the stationary phase

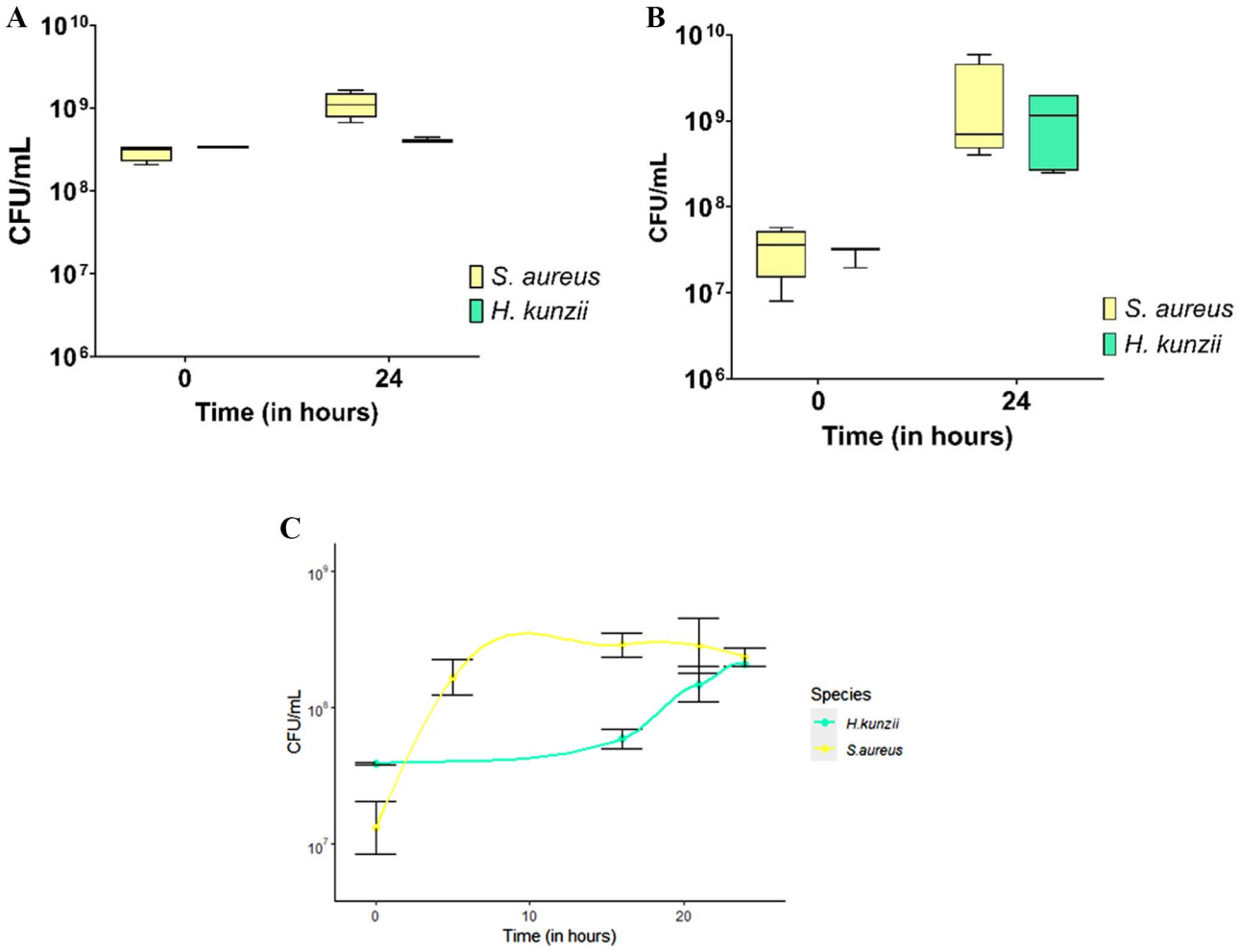

Fig. 1 Growth kinetics of coculture experiment. This figure presents the endpoint CFU counts at 0 and 24 h for *S. aureus* and *H. kunzii*, with the initial OD_{600} set at **A**. 1 and **B**. 0.1. **C**. Growth curves in coculture (with an initial inoculum OD600 of 0.1) of *S. aureus* and *H. kunzii* over a 24 h period. The initial ratio was set at 1:3 in favour of *H. kunzii* to achieve an equal quantity of bacteria at 21 h. The curves were smoothed using a linear model, with each point representing CFU counts according to time in hours. Colonies grown on TSS were differentiated based on their morphology: *H. kunzii* colonies appeared as pinhead translucent grey, while *S. aureus* formed hemolytic, yellowish, and larger ones. In addition, the CFU counts of *S. aureus* were compared between LB and TSS agar medium

(activation phase of the *agr* system and production of virulence factors in *S. aureus*). At 24 h, each strain was present in the same proportion (2 10^8 CFU/mL, in both mono and coculture), enabling a comparison of these two conditions in term of protein production.

Downregulation of *agrA* in *S. aureus* in the presence of *H. kunzii* Exoproteome

As previously reported, *H. kunzii* can modulate the virulence of *S. aureus* by downregulating the transcription of the *agrA* gene [10]. The expression of *agrA* in *S. aureus* was monitored in two ways: (i) post-coculture, and (ii) after exposure to the *H. kunzii* exoproteome (MEHkE). The aim was to validate the hypothesis of a contact-independent interaction between the two species, which is sufficient to induce the downregulation of *agrA* gene expression and reduce the virulence of *S. aureus*.

Under all conditions tested, we observed a consistent decrease in *agrA* expression (Fig. 2). Notably, this reduction was statistically significant ($p<0.05$) when *S. aureus*, in the stationary phase ($OD_{600}=1$), was exposed to MEHkE. This observation supports the notion that *H. kunzii* H13 may secrete proteins that downregulate the expression of *agrA* in *S. aureus*.

Identification of candidate *H. kunzii* secreted proteins decreasing *S. aureus* virulence

To identify the proteins secreted by *H. kunzii*, whether in the presence or absence of *S. aureus*, we conducted a proteomic study under two conditions: an initial inoculum of *H. kunzii and S. aureus* at $OD_{600}=1$ (interaction during only the stationary phase) and $OD_{600}=0.1$ (interaction during both the exponential and stationary phases). *H. kunzii* alone secreted a limited number of proteins at

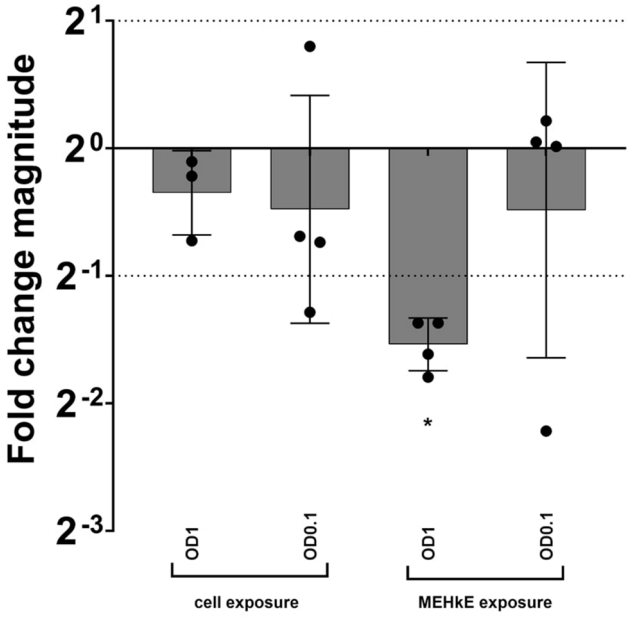

Fig. 2 Level of *agrA* gene expression in *Staphylococcus aureus* after a 24 h exposure to either *Helcococcus kunzii* cells (in coculture) or MEHkE (a protein extract from the supernatant of *H. kunzii* culture media). The Initial inoculum of *S. aureus* was set at an OD_{600} of 1 (for the stationary phase), and an OD_{600} of 0.1 (for both the exponential and stationary phases). MEHkE refers to a medium enriched with the exoproteome of *H. kunzii*. A *p-value* < 0.05 is indicated by *

all stages of its growth (n=42 at OD_{600}=1 and n=44 at OD_{600}=0.1). A similar limited number of secreted proteins was also described in the presence of *S. aureus* (n=55 at OD_{600}=1 and n=18 at OD_{600}=0.1) (Figure S2).

Given the significant downregulation of *agrA gene* expression observed after exposure to MEHkE, we searched for proteins secreted by *H. kunzii* that interact with *S. aureus.* As the *agr* system is activated at the end of the exponential phase and sustained throughout the stationary phase [11], proteins interacting with this system are potentially secreted by *H. kunzii* during the stationary phase. Among the initial list of 75 proteins recovered from the *H. kunzii* exoproteome, 55 belonged to the exoprotein fraction from coculture at OD_{600}=1, corresponding to this stationary phase. Of these 55 candidates, 17 were associated with transcriptional activity, including eight ribosomal subunits. Surprisingly, RsmB (Ribosomal Subunit B) (GUI37_RS04270), a genomic candidate previously identified [12], was found only in the proteome and not in the exoproteome. In addition, 17 of the 55 exoproteins found were linked to carbohydrate metabolism, including the type 3 glyceraldehyde-3-phosphate dehydrogenase protein (GPAH), already described as protein with variable independent biological activities [30]. At OD_{600}=0.1 (both exponential and stationary phases), 18 proteins candidates were identified. Ultimately, 16 proteins were definitively included because they were present in all conditions (Table 1). Interestingly, four of these proteins were associated with a potential to alter cell wall architecture: the polysaccharide deacetylase family protein (WP_212661168.1), peptidoglycan DD-metalloendopeptidase family protein (WP_212661263.1), and the aforementioned type I GPAH (WP_005397984.1 and WP_005398187.1). Two of the 16 proteins included presented a stronger interest: the trypsin-like peptidase domain-containing protein (WP_212661130.1) with a serine protease domain, previously described for their potential in *S. aureus-S. epidermidis* interaction [31] and the extracellular solute-binding protein (WP_212660510.1), which could impact nutritional competition [32].

Table 1 List of proteins secreted by *Helcococcus kunzii* under all conditions. These conditions include an OD600 of 0.1, where both strains underwent the exponential growth phase and reached the stationary growth phase, and an OD600 of 1, where both strains remained continuously in the stationary phase. The proteins listed in this table show the most potential for attenuating the virulence of *S. Aureus*

Locus_tag	Protein_id	Protein
GUI37_RS00090	WP_005396836.1	hypothetical protein
GUI37_RS00890	WP_005397107.1	formate C-acetyltransferase
GUI37_RS01090	WP_212661130.1	trypsin-like peptidase domain-containing protein
GUI37_RS01425	WP_212661168.1	polysaccharide deacetylase family protein
GUI37_RS01930	WP_212661252.1	2-dehydropantoate 2-reductase
GUI37_RS02030	WP_212661263.1	peptidoglycan DD-metallo-endopeptidase family protein
GUI37_RS02985	WP_005397814.1	HU family DNA-binding protein
GUI37_RS03540	WP_005397984.1	type I glyceraldehyde-3-phosphate dehydrogenase
GUI37_RS03545	WP_212661385.1	phosphoglycerate kinase
GUI37_RS03555	WP_005397990.1	2,3-bisphosphoglycerate-independent phosphoglycerate mutase
GUI37_RS03560	WP_005397992.1	phosphopyruvate hydratase
GUI37_RS04205	WP_005398187.1	type I glyceraldehyde-3-phosphate dehydrogenase
GUI37_RS05200	WP_212660510.1	extracellular solute-binding protein
GUI37_RS06220	WP_212660639.1	flavocytochrome c
GUI37_RS07030	WP_212660710.1	hypothetical protein
GUI37_RS07980	WP_005399120.1	IMP dehydrogenase

Shortlisted candidates are highlighted in gray

H. kunzii exoproteome impacts regulation of S. aureus virulence factors during stationary growth phase

To investigate the influence of the *H. kunzii* exoproteome on *S. aureus* virulence, we focused on the regulatory gene network that governs *S. aureus* during stationary growth phase (OD=1) (Fig. 3).

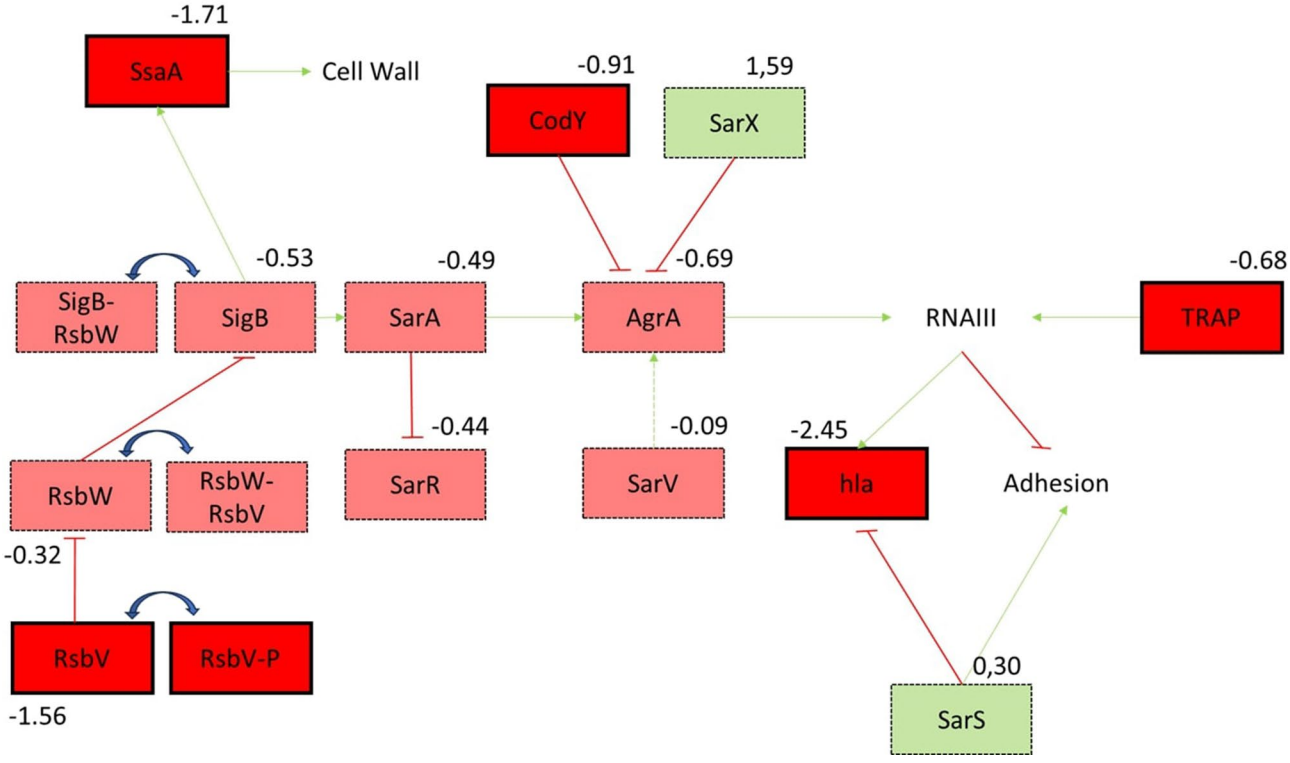

Fig. 3 Regulatory network of *S. aureus* virulence within the proteome fraction of the stationary growth phase (OD1). Triangle shape arrows in green indicate activating interactions, while blunt head arrows in red indicate inhibiting activity. Blue double-headed arrows represent the dynamics of protein complexation. Proteins are depicted in boxes with solid black borders (to denote statistical significance), or dashed borders (to indicate trends). Red-filled boxes indicate proteins less produced in coculture, whereas green-filled boxes denote proteins with increased production. The associated $\log_2$ fold change (FC) values are presented above each box

The production of both the RNAIII-activating regulator AgrA (NWMN_1946) and the RNAIII-activating protein TRAP (NWMN_1726) was reduced, with TRAP showing a significant reduction ($p=0.0068$). The log2 fold change (log2FC) for AgrA and TRAP was −0.69 and −0.68, respectively. Both proteins are associated with the induction of RNAIII, a stable regulatory RNA that enhances hemolysin production [33].

Previous studies have indicated that AgrA production could be positively regulated by SarA (NWMN_0588) and SarV (NWMN_2167), and negatively regulated by SarX (NWMN_0637) and CodY (NWMN_1165) [34–36]. In coculture experiments, the production of SarA and SarV was non-significantly reduced ($\log_2$FC= -0.49, p=not significant (NS) and $\log_2$FC =-0.09, p=NS, respectively), potentially accounting for the decrease in AgrA production. Interestingly, the production of CodY was also significatively reduced in coculture experiments ($\log_2$FC= -0.91, $p=0.0269$) while SarX, another negative regulator of AgrA, was non-significatively increased ($\log_2$FC=1.59, p=NS). In summary, the virulence regulatory network of *S. aureus* appears to be impaired upon coculture potentially explaining a significant intracellular reduction of alpha hemolysin production (NWMN_1073, Log2FC=-2.45, $p=0.0079$)).

Additionally, the regulatory network of the stress response pathway was also affected. The production of Sigma B (NWMN_1970) was non-significantly reduced in coculture ($\log_2$FC=-0.53, $p=0.1430$), as well as the production of its repressor, the anti-sigmaB, RsbW (NWMN_1971) with a $\log_2$FC=-0.32 ($p=0.0869$). Sigma B is inactivated when it complexes with RsbW, this inactivated form loses the ability to bind DNA and exert its role as transcriptional regulator. Furthermore, the production of the anti-RsbW factor, RsbV (NWMN_1972), leads to the liberation of the free form of SigmaB. The coculture induced a significant reduction in RsbV production, which would translate into a reduced potential to find the free and thus active form of Sigma B (Fig. 3).

To corroborate these findings, we tested several virulence genes that are supposed to be regulated by *agrA* expression in *S. aureus* using qRT-PCR after coculture with *H. kunzii* **(Fig S3)**. The genes tested included *hla* and *sarA*, which are up-regulated by RNAIII, and *spa* and *sigB*, which are down-regulated by *agr*. As anticipated, we observed a significant downregulation of *hla* ($p<0.0001$) and *sarA* ($p<0.01$) in NSA739 when associated with H13. Consequently, the *sigB* and *spa* genes demonstrated a significant overexpression in the presence of *H. kunzii* H13 ($p<0.01$).

Virulence factors with cytolytic activity need to be secreted, particularly during the stationary phase. Therefore, we investigated the exoproteome fraction of *S. aureus* in this phase. In coculture, only two proteins were statistically less produced: a threonyl-tRNA synthetase (NWMN_1576) and an ATP-binding subunit ClpC (NWMN_2448), with a log_2FC of -1.92 ($p=0.0048$) and −2.69 ($p=0.0020$), respectively. The presence of the *H. kunzii* exoproteome impacted some virulence effectors. The production of gamma hemolysin components ABC (NWMN_2318-2320-2319, log_2FC=-0.82, -1.2, -0.82 respectively; p=NS), leukocidin/hemolysin toxin family F (NWMN_1927, log_2FC=-1.53; p=NS) and S (NWMN_1928, log_2FC=-1.42; p=NS) subunits, as well as the alpha hemolysin precursor (NWMN_1073, log_2FC=-0.36; p=NS), were non-significantly reduced in the exoproteome fraction of the coculture.

To determine whether this decrease in virulence factors from the exoproteome was associated with a defect in their production or export, we analyzed the proteomic fraction. As mentioned earlier, the production of the alpha hemolysin precursor was significantly reduced in the proteomic fraction, with a log_2FC=-2.45 ($p=0.0079$), explaining the reduced production of alpha hemolysin in the exoproteome. However, the production of leukocidin/hemolysin toxin family F (log_2FC=0.62; p=NS) and S (log2FC=0.30; p=NS) subunits and gamma hemolysin component B (log2FC=0.24; p=NS) were increased upon coculture within the proteome. This suggests that they are either retained intracellularly or that their stability was affected once they were released extracellularly.

S. aureus hemolysin production is reduced in the presence of *H. kunzii*

In order to investigate the influence of *H. kunzii* on the production of hemolysin by *S. aureus*, we conducted a test for hemolysin production. This involved comparing the hemolytic capacity of *S. aureus* alone and in coculture with *H. kunzii*. As depicted in Figure S4, the hemolytic activity was observed in 100% of the monocultured *S. aureus* (Figures S4A and B). In contrast, the coculture exhibited a significant decrease in hemolysin production in the presence of *H. kunzii* ($p<0.0001$) (Figures S4A and C). This suggests that the virulence of *S. aureus* is altered by the exoproteome of *H. kunzii*, and this modification occurs independently of the *agr system.*

S. aureus virulence is modified by *H. kunzii* exoproteome independently of the *agr system*

As previously established, bacteria acquire iron through ABC transport, transferrin binding, or siderophore production to sustain their metabolism [37]. Our study, as revealed by KEGG analysis, shows that one *S. aureus* siderophore biosynthetic pathway was impeded by two proteins (NWMN_2080-82, SfnaB and D, respectively) involved in the conversion of D-ornithine to staphyloferrin A [38]. More specifically, the biosynthesis of staphyloferrin A involves a cascade of enzymatic reactions, starting with the metabolite 2-oxaloglutarate as a precursor. This precursor goes through D-ornithine to finally be converted into staphyloferrin A, a process that requires the aforementioned SfnaBD enzyme (**Figure S5A**). These proteins were only detected in monoculture samples. Additionally, a staphyloferrin precursor, 2-oxaloglutarate, previously described to be produced by the citrate cycle through acetate oxidation (TCA) [39, 40], was also affected in its biosynthetic pathway, with the entire TCA being negatively impacted in coculture (**Figure S5B**). We also observed that the production of six proteins involved in iron metabolism were significantly impacted in the coculture experiment. The production of Ferrochelatase (NWMN_1724) was enhanced (log_2FC=0.77; $p=0.030$), while the production of five others was decreased: the iron compound ABC transporter, the iron compound-binding protein (NWMN_2185, log_2FC=-1.37; $p=0.0045$, and NWMN_0581, log_2FC=-2.73; $p=0.0007$), the siderophore compound ABC transporter binding protein (NWMN_0059, log_2FC=-2.24; $p=0.0006$), and two ferrichrome ABC transporter lipoproteins (NWMN_2078, log_2FC=-2.16, $p=0.0003$ and NWMN_0705, log_2FC=-5.23; $p=0.0002$). The latter exhibited the most significant decrease in the coculture experiment.

Finally, proteins involved in cell wall formation and virulence effectors of *S. aureus* were directly inhibited (Figure S6). The cell wall formation was affected at the biosynthesis level of wall teichoic and lipoteichoic acids, with the production of TagAE, TarL, and LtaS found exclusively in monoculture samples (Figure S6A). Moreover, staphyloxanthin production (Figure S6B), a protein protecting *S. aureus* from neutrophils clearance [41, 42], was impaired due to the absence of CrtM and CrtP enzymes in coculture samples (Figure S6B).

Impact of *H. kunzii* exoproteome on *S. aureus* metabolism

Upon exposure to *H. kunzii* exoproteome, the protein production capability of *S. aureus* was reduced. This is evidenced by the higher absolute diversity of proteins recovered from monoculture samples compared to those from coculture. Furthermore, the coculture in the stationary phase exhibited the lowest diversity of *S. aureus* proteins (Fig. 4). Out of the 775 proteins identified during the stationary phase, which constitute the *S. aureus* proteome under coculture conditions, 315 (40.6%) were significantly differentially produced (p-values ranged from 0.00023 to 0.2651, with the latter achieving significance through Perseus statistical treatment). Among these differentially produced proteins, only 10 (1.3%) were overproduced in

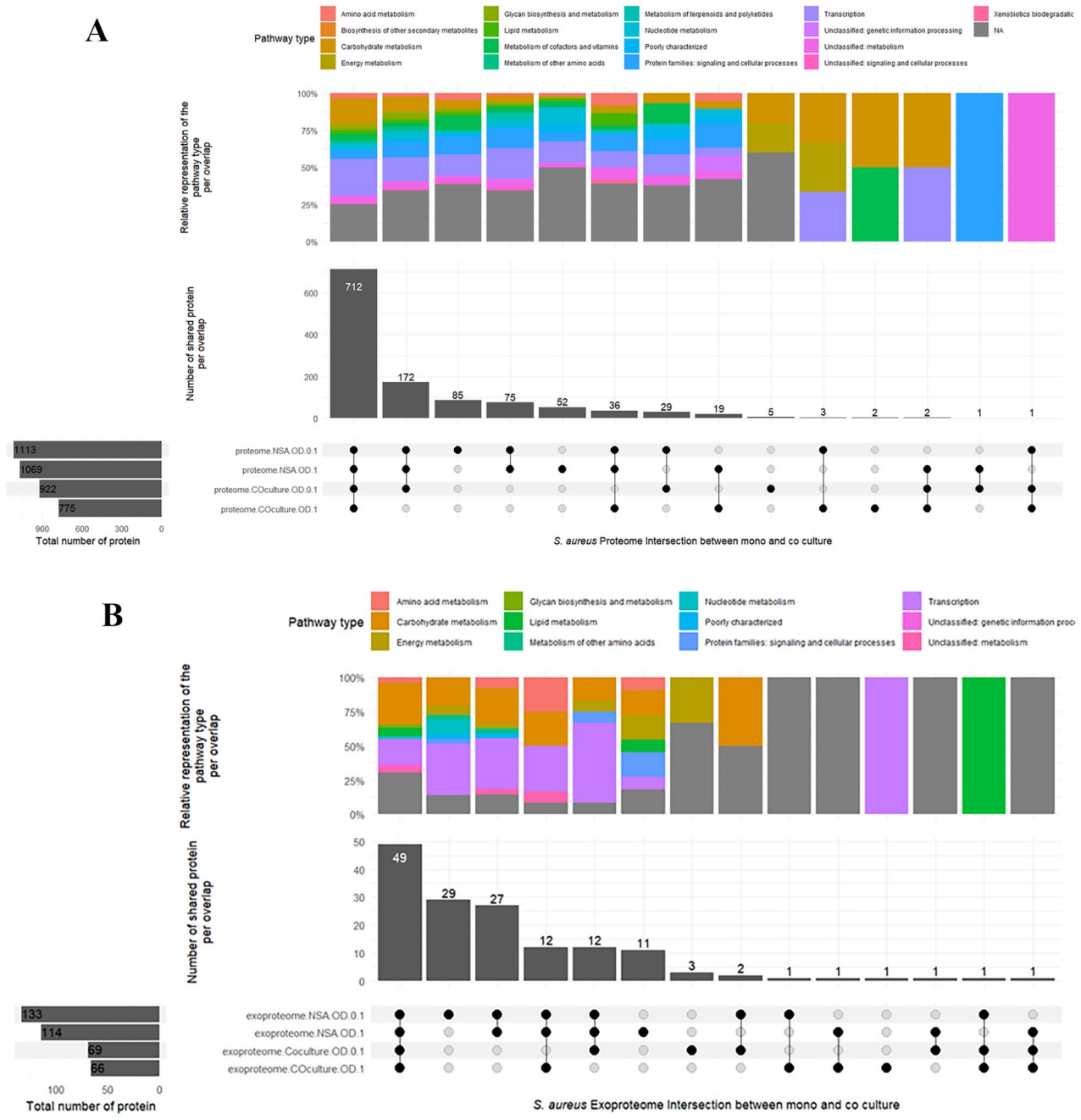

Fig. 4 Distribution of proteins in proteome (**A**) and exoproteome (**B**) of *Staphylococcus aureus* and their associated pathways. It compares the proteome and exoproteome of *S. aureus* identified at the exponential (OD600 = 0.1) and stationary (OD600 = 1) phases of growth in both mono-culture (NSA) and coculture conditions. The data are visualized using an UpSet matrix layout and plotted horizontally. Each column in the layout represents a set of proteins, indicated by the dark circles, and illustrates the associated pathways

the coculture. This underscores the potential of *H. kunzii* presence to repress metabolic activity.

Discussion

The results from our clinical and microbiological observations corroborate the in vivo findings obtained previously, suggesting a potential interaction between *S. aureus* and *H. kunzii* in chronic wounds, particularly in diabetic foot ulcers. The frequent co-isolation of these two species underscores their proximity within the wound bed [9]. Our prior study demonstrated a phenotypic variation in *S. aureus* when cocultured with *H. kunzii* [10]. This commensal bacterium was found to reduce the virulence of *S. aureus* in an *in vivo C. elegans* model

[10] by acting on the *agr* system, a key regulator of virulence. Building on these findings, the aim of this study was to replicate the environmental conditions in an in vitro model that lead to a decrease in *S. aureus* virulence in the presence of *H. kunzii*, and to identify the proteins involved in this molecular interaction.

To investigate the in vitro molecular interactions between *S. aureus* and *H. kunzii*, we utilized CWM [15]. In traditional in vitro experiments, bacteria are typically cultured in an artificial medium, which significantly differs from the clinical environment. This discrepancy can influence bacterial virulence and often limits the clinical relevance of the findings. The use of CWM, designed to mimic the environmental conditions of a chronic wound (including the presence of blood and serum), was crucial for facilitating the growth of *H. kunzii* in a liquid medium. This contrasts with traditional culture media like LB media, which do not support the growth of *H. kunzii*. Our results confirm that *S. aureus* and *H. kunzii* can coexist and proliferate together in this environment, overcoming challenges observed in other studies focusing on bacterial interactions. Notably, studies investigating interactions between *S. aureus* and *Pseudomonas aeruginosa* have reported difficulties in coculturing them in vitro, thereby hindering a comprehensive understanding of their interaction [43]. So, Traditional culture media were found to obstruct the simultaneous growth of *P. aeruginosa* and *S. aureus* [43]. In such an artificial environment, bacteria primarily compete for nutrients like iron, leading to the dominance of one species over the other. We have previously demonstrated that CWM enables the concurrent growth of *P. aeruginosa* and *S. aureus* without either species dominating [15]. The feasibility of coculturing *H. kunzii* and *S. aureus* in this medium is confirmed in this study.

Further analysis of the growth curves revealed that, despite *H. kunzii* exhibiting a delayed exponential phase, both *S. aureus* and *H. kunzii* reached the stationary phase in similar proportions after 24 h. The growth curves suggested that *H. kunzii* only enters its exponential phase once *S. aureus* has reached the stationary phase. This indicates that *H. kunzii* could potentially utilize resources (such as nutrients) and space once *S. aureus* ceases to multiply [44, 45].

Moreover, we found that exposure to the secreted proteome of *H. kunzii* significantly reduced the expression of the *agrA* gene in vitro. This finding aligns with our previous in vivo results and is particularly noticeable when *S. aureus* is in the stationary phase. Given that the *agr system* is activated during the late exponential phase and maintains a lower level during the stationary phase (first 6–7 h) [11], this interaction likely impacts the maintenance of the *agr* loop rather than its initial activation [11]. This effect on the *agr system* is more pronounced after exposure to MEHkE than in coculture, as previously demonstrated by Ramsey et al.. These authors highlighted that exposure to the culture supernatant of *Corynebacterium striatum* was sufficient to alter the expression of Agr-dependent genes in *S. aureus* during the stationary phase [17].

We further investigated the potential molecular interactions between *H. kunzii* and *S. aureus* through an exoproteome analysis, which identified several candidate proteins that could explain the interaction (Table 1). For instance, GPAH, previously described in *Lactobacillus* as causing cell wall damage [17, 46] and playing a role in iron uptake, may also contribute to the interaction between *H. kunzii* and *S. aureus* [47]. Additionally, proteins such as the peptidoglycan DD-metalloendopeptidase family protein and polysaccharide deacetylase family protein, both implicated in membrane damage, suggest a redundant activity. The combined catalytic activities of these proteins could impair membrane function, potentially inducing a stress response that contributes to the alteration of virulence factors regulation. The remaining potential targets, a trypsin-like peptidase domain-containing protein and an extracellular solute-binding protein, may also adversely affect cell wall function and compete for resources. As mentioned in previous publications, extracellular serine proteases have already been described as being involved in the interaction between *S. aureus* and *S. epidermidis*, with a negative impact on biofilm formation [31] and cell wall-associated proteins [48]. The extracellular solute-binding protein is also an interesting candidate, as solute binding proteins are involved in nutrient acquisition, potentially leading to alterations in *S. aureus* feeding behaviour [32, 49].

Shifting our focus to the regulatory network of *S. aureus* virulence (Fig. 3), we observed a significant reduction in the production of TRAP and AgrA (RNA III activators), leading to a decrease in alpha hemolysin production. However, the regulatory network governing alpha hemolysin production showed some inconsistencies. For instance, CodY, which is expected to negatively influence virulence factor production, was found in lower abundance in the coculture at the stationary phase. However, its involvement appears to be most relevant during the exponential phase [35]. The stress response SigmaB regulon also appeared to be altered, with the production of SigmaB and its regulators being reduced. SigmaB, known for its pleiotropic role, plays a central role in adaptation [50], impacting virulence factor production through the activation of SarA, which in turn activates AgrA [51]. As previously described, the transcriptional activity of Sigma B is dependent on the phosphorylation status of RsbV; only the unphosphorylated RsbV can release Sigma B from RsbW [52]. Sigma B is associated with osmotic stress [53] and cell wall alteration, as a

result of the inhibition of the wall teichoic acid synthesis pathway, has been linked to osmotic stress [54–56]. The overall result is a disruption in the regulation factor coordinating virulence factor production. These results have been confirmed by the evaluation of the expression of these genes by qRT-PCR and by a hemolysis test.

Several metabolic pathways of *S. aureus* were impacted by the interaction with *H. kunzii*, particularly during the stationary phase. For instance, the production of staphyloxantin and staphyloferrin, proteins involved in staphylococcal virulence [57], were repressed. These proteins play a direct role in escaping the immune system response (Reduction of Oxidative Stress, ROS) and facilitating iron uptake [57, 58]. Nutrient uptake, especially co-factors like iron, is a limiting factor in bacterial virulence [58], particularly in *S. aureus* through *fur* regulation [59]. Cell wall components of *S aureus*, including wall teichoic and lipoteichoic acids, were also affected. These alterations can impact both virulence [60, 61] and surface colonization (D-alanin incorporation) [62]. The collective results suggest a metabolically repressed state of *S. aureus* when associated with *H. kunzii*. The profound remodeling of the *S. aureus* proteome, indicated by a decrease in proteomic diversity during coculture, suggests an adaptation to the presence of *H. kunzii*. A total of 279 proteins were no longer produced at an OD600 of 1 in coculture with *H. kunzii* compared to *S. aureus* monoculture, with 212 associated with the proteomic fraction and 67 with the exoproteome (Fig. 4). Additionally, the exoproteome of *S. aureus* has been extensively studied under various conditions [64, 65], revealing a range of proteins identified from 186 to 1404. These proteins are predominantly associated with virulence, metabolism, and carbohydrate functions [62]. Aligning the reconstructed pathways revealed that those affected at an OD600 of 0.1 were even more impacted at an OD600 of 1. This suggests that the fine-tuning of *S. aureus* metabolism is more affected after reaching the stationary state. This could be attributed to impaired nutrient and cofactor uptake, highlighting the tight connection between metabolic capacities and virulence [32].

Conclusion

This study offers valuable insights into the in vitro molecular interactions between *S. aureus* and *H. kunzii*, elucidating the mechanism that leads to a reduction in *S. aureus* virulence when *H. kunzii* is present. The findings shed light on the potential proteins involved in this interaction at a molecular level, unraveling a complex interplay that influences the regulatory network and overall metabolism of *S. aureus*. The decrease in *S. aureus* virulence is not linked to cell-cell contact, but is primarily dependent on proteins secreted by *H. kunzii*. Our proteomic approach suggests that these secreted proteins may be involved in attenuating virulence, which is associated with a significant metabolic remodeling that alters the *S. aureus* virulence regulatory network. Finally, we identified a shortlist of six proteins produced by *H. kunzii* that hold high potential for anti-virulence therapy. Future investigations will explore the phenotypic impact of the excreted factors potentially involved in this virulence modulation. This work contributes to a better understanding of the dynamics between bacterial species in chronic wound environments, laying the groundwork for further research into therapeutic interventions and strategies for managing diabetic foot infections.

Abbreviations

CFU	Colony Forming Unit
CWM	Chronic Wound Medium
FC	Fold Change
GPAH	Glyceraldehyde-3-phosphate dehydrogenase
LDS	Lithium duodecylsulfate
LBA	Luria Bertani broth Agar
MEHkE	Medium enriched with H. kunzii exoproteome
NS	Not significant
OD	Optical density
RsmB	Ribosomal Subunit B
RT-qPCR	Retrotranscription quantitative PCR
ST	Sequence type
TCA	Through acetate oxidation
TRAP	Translocon-associated protein
TTE	Tris Triton EDTA
TSS	Trypticase Soy supplemented with 5% sheep blood

Supplementary Information

The online version contains supplementary material available at https://doi.org/10.1186/s12866-024-03520-0.

Supplementary Material 1

Supplementary Material 2

Supplementary Material 3

Supplementary Material 4

Supplementary Material 5

Supplementary Material 6

Supplementary Material 7

Supplementary Material 8

Supplementary Material 9

Supplementary Material 10

Supplementary Material 11

Acknowledgements

We thank the Nîmes University hospital for its structural, human and financial support through the award obtained by our team during the internal call for tenders « Thématiques phares ». We thank Sarah Kabani for her editing assistance.

Author contributions

BARND conducted all experiments and wrote the manuscript. RD conducted new experiments. BARND and LG conducted the proteomic experiments. MM conducted genomic analysis. JA, JPL and CDR conceived and designed the experiments. All authors have read the article and approved the submitted version.

Funding
This research was funded by CHU Nîmes, grant number: Thematique Phare 1. The funder had no role in study design, data collection and analysis, decision to publish or preparation of the manuscript.

Data availability
The genomic data are available on the NCBI GenBank database under the BioProject number: PRJNA1078120 and BioSample: SAMN43517085, Accession: CP169293, Genomes: Staphylococcus aureus NSA 739. The mass spectrometry proteomics data have been deposited to the ProteomeXchange Consortium via the PRIDE partner repository with the dataset identifier PXD049416 and 10.6019/PXD049416. This dataset is accessible for the reviewers using the username reviewer_pxd049416@ebi.ac.uk and the password 0qZ91Ona [66].

Declarations

Ethics approval and consent to participate
All strains used in this study belonged to the collection of the Department of Microbiology at Nîmes University Hospital (France). The study was submitted to the Institutional Review Board (IRB) of Nîmes University Hospital, France. The IRB deemed it unnecessary to obtain consent to participate from patients in accordance with national regulation. This is because the analysis of biological samples was conducted in the context of medical care and was considered as non-interventional research. Furthermore, this study utilized only bacterial strains and did not involve human specimens or the exploration of clinical data. In this context, the IRB determined that only the non-opposition of the patient during sampling was required, in accordance with articles L1221-1.1, L1211-2, and N°DC-2020-4155 of the French Public Health Code. Consequently, the requirement for consent to participate was waived by the IRB of Nîmes University Hospital.

Consent for publication
Not applicable.

Competing interests
The authors declare no competing interests.

Received: 17 May 2024 / Accepted: 13 September 2024
Published online: 11 October 2024

References

1. Järbrink K, Ni G, Sönnergren H, Schmidtchen A, Pang C, Bajpai R, et al. The humanistic and economic burden of chronic wounds: a protocol for a systematic review. Syst Rev. 2017. https://doi.org/10.1186/s13643-016-0400-8.
2. Dowd SE, Wolcott RD, Sun Y, McKeehan T, Smith E, Rhoads D. Polymicrobial Nature of Chronic Diabetic Foot Ulcer Biofilm infections determined using bacterial tag encoded FLX Amplicon Pyrosequencing (bTEFAP). PLoS ONE. 2008. https://doi.org/10.1371/journal.pone.0003326.
3. Johani K, Malone M, Jensen S, Gosbell I, Dickson H, Hu H, et al. Microscopy visualisation confirms multi-species biofilms are ubiquitous in diabetic foot ulcers. Int Wound J. 2017. https://doi.org/10.1111/iwj.12777.
4. Durand BARN, Pouget C, Magnan C, Molle V, Lavigne J-P, Dunyach-Remy C. Bacterial interactions in the Context of Chronic Wound Biofilm: a review. Microorganisms. 2022a. https://doi.org/10.3390/microorganisms10081500.
5. Wolcott RD, Hanson JD, Rees EJ, Koenig LD, Phillips CD, Wolcott RA, et al. Analysis of the chronic wound microbiota of 2,963 patients by 16S rDNA pyrosequencing. Wound Repair Regen. 2016. https://doi.org/10.1111/wrr.12370.
6. Wolcott R. Disrupting the biofilm matrix improves wound healing outcomes. J Wound Care. 2015. https://doi.org/10.12968/jowc.2015.24.8.366.
7. Pouget C, Dunyach-Remy C, Pantel A, Schuldiner S, Sotto A, Lavigne JP. Biofilms in Diabetic Foot Ulcers: significance and clinical relevance. Microorganisms. 2020. https://doi.org/10.3390/microorganisms8101580.
8. Dunyach-Remy C, Ngba Essebe C, Sotto A, Lavigne JP. *Staphylococcus aureus* Toxins and Diabetic Foot Ulrole: Role in Pathogenesiinterestterediagnosis-gnosis. Toxins. 2016. https://doi.org/10.3390/toxins8070209.
9. Vergne A, Guérin F, Lienhard R, Le Coustumier A, Daurel C, Isnard C, et al. In vitro antimicrobial susceptibility of *Helcococcus kunzii* and molecular analysis of macrolide and tetracycline resistance. Eur J Clin Microbiol Infect Dis. 2015. https://doi.org/10.1007/s10096-015-2451-5.
10. Ngba Essebe C, Visvikis O, Fines-Guyon M, Vergne A, Cattoir V, Lecoustumier A, et al. Decrease of *Staphylococcus aureus* Virulence by *Helcococcus kunzii* in a *Caenorhabditis elegans* Model. Front Cell Infect Microbiol. 2017;7. https://doi.org/10.3389/fcimb.2017.00077.
11. Grundstad ML, Parlet CP, Kwiecinski JM, Kavanaugh JS, Crosby HA, Cho Y-S, et al. Quorum sensing, virulence, and Antibiotic Resistance of USA100 Methicillin-Resistant Staphylococcus *aureus* isolates. mSphere. 2019. https://doi.org/10.1128/mSphere.00553-19.
12. Durand BARN, Yahiaoui Martinez A, Baud D, François P, Lavigne J-P, Dunyach-Remy C. Comparative genomics analysis of two *Helcococcus kunz*ii strains co-isolated with Staphylococcus *aureus* from diabetic foot ulcers. Genomics. 2022b. https://doi.org/10.1016/j.ygeno.2022.110365.
13. Durand BARN, Dunyach-Remy C, El Kaddouri O, Daher R, Lavigne JP, Armengaud J, Grenga L. Proteomic insights into Helcococcus kunzii in a diabetic foot ulcer-like environment. Proteom Clin Appl 2023. https://doi.org/10.1002/prca.202200069
14. Sotto A, Lina G, Richard JL, Combescure C, Bourg G, Vidal L, et al. Virulence potential of *Staphylococcus aureus* strains isolated from Diabetic Foot Ulcers: a new paradigm. Diabetes Care. 2008. https://doi.org/10.2337/dc08-1010.
15. Pouget C, Dunyach-Remy C, Bernardi T, Provot C, Tasse J, Sotto A, et al. A relevant Wound-Like in vitro media to Study Bacterial Cooperation and Biofilm in Chronic wounds. Front Microbiol. 2022. https://doi.org/10.3389/fmicb.2022.705479.
16. Wessel D, Flügge UI. A method for the quantitative recovery of protein in dilute solution in the presence of detergents and lipids. Anal Biochem. 1984. https://doi.org/10.1016/0003-2697(84)90782-6.
17. Ramsey MM, Freire MO, Gabrilska RA, Rumbaugh KP, Lemon KP. *Staphylococcus aureus* Shifts toward Commensalism in Response to *Corynebacterium* Species. Front. Microbiol. 2016. https://doi.org/10.3389/fmicb.2016.01230
18. Pouget C, Gustave CA, Ngba-Essebe C, Laurent F, Lemichez E, Tristan A, et al. Adaptation of *Staphylococcus aureus* in a medium mimicking a Diabetic Foot Environment. Toxins. 2021. https://doi.org/10.3390/toxins13030230.
19. Garzoni C, Francois P, Huyghe A, Couzinet S, Tapparel C, Charbonnier Y, et al. A global view of *Staphylococcus aureus* whole genome expression upon internalization in human epithelial cells. BMC Genomics. 2007. https://doi.org/10.1186/1471-2164-8-171.
20. Labandeira-Rey M, Couzon F, Boisset S, Brown EL, Bes M, Benito Y et al. Staphylococcus aureus Panton-Valentine Leukocidin Causes Necrotizing Pneumonia. Science. 2007. https://doi.org/10.1126/science.1137165
21. Sihto HM, Tasara T, Stephan R, Johler S. Validation of reference genes for normalization of qPCR mRNA expression levels in *Staphylococcus aureus* exposed to osmotic and lactic acid stress conditions encountered during food production and preservation. FEMS Microbiol Lett. 2014. https://doi.org/10.1111/1574-6968.12491.
22. Livak KJ, Schmittgen TD. Analysis of relative gene expression data using real-time quantitative PCR and the 2 – ΔΔCT method. Methods. 2001. https://doi.org/10.1006/meth.2001.1262.
23. Magnan C, Ahmad-Mansour N, Pouget C, Morsli M, Huc-Brandt S, Pantel A, et al. Phenotypic and genotypic virulence characterisation of *Staphylococcus pettenkoferi* strains isolated from Human Bloodstream and Diabetic Foot infections. Int J Mol Sci. 2022. https://doi.org/10.3390/ijms232415476.
24. Lê S, Josse J, Husson F, FactoMineR. A Package for Multivariate Analysis. J Stat Softw. 2008. https://doi.org/10.18637/jss.v025.i01.
25. Weijun L. Pathview: an R/Bioconductor package for pathway-based data integration and visualization. Bioinformatics. 2013. https://doi.org/10.1093/bioinformatics/btt285.
26. Gu Z, Eils R, Schlesner M. Complex heatmaps reveal patterns and correlations in multidimensional genomic data. Bioinformatics. 2016. https://doi.org/10.1093/bioinformatics/btw313.
27. Kassambara A, Mundt F. Factoextra: Extract and Visualize the Results of Multivariate Data Analyses. 2020. https://CRAN.Rproject.org/package=factoextra
28. Core Team R. R: A Language and Environment for Statistical Computing. Vienna, Austria: R Foundation for Statistical Computing. 2021. https://www.R-project.org/
29. Tyanova S, Temu T, Sinitcyn P, Carlson A, Hein MY, Geiger T, et al. The Perseus computational platform for comprehensive analysis of (prote)omics data. Nat Methods. 2016. https://doi.org/10.1038/nmeth.3901.
30. Boradia VM, Raje M, Raje CI. Protein moonlighting in iron metabolism: glyceraldehyde-3-phosphate dehydrogenase (GAPDH). Biochem Soc Trans. 2014. https://doi.org/10.1042/BST20140220.

31. Iwase T, Uehara Y, Shinji H, Tajima A, Seo H, Takada K, et al. *Staphylococcus epidermidis* Esp inhibits *Staphylococcus aureus* biofilm formation and nasal colonization. Nature. 2010. https://doi.org/10.1038/nature09074.
32. Richardson AR, Virulence. Metabolism Microbiol Spectr. 2019. https://doi.org/10.1128/microbiolspec.GPP3-0011-2018.
33. Morfeldt E, Taylor D, von Gabain A, Arvidson S. Activation of alpha-toxin translation in *Staphylococcus aureus* by the trans-encoded antisense RNA, RNAIII. EMBO J. 1995. https://doi.org/10.1002/j.1460-2075.1995.tb00136.x.
34. Manna AC, Cheung AL. Expression of SarX, a negative Regulator of agr and Exoprotein Synthesis, is activated by MgrA in *Staphylococcus aureus*. J Bacteriol. 2006. https://doi.org/10.1128/JB.00297-06.
35. Majerczyk CD, Sadykov MR, Luong TT, Lee C, Somerville GA, Sonenshein AL. *Staphylococcus aureus* CodY Negatively Regulates Virulence Gene Expression. J Bacteriol. 2008. https://doi.org/10.1128/JB.01545-07
36. Reyes D, Andrey DO, Monod A, Kelley WL, Zhang G, Cheung AL. Coordinated regulation by AgrA, SarA, and SarR to control *agr* expression in *Staphylococcus aureus*. J Bacteriol. 2011. https://doi.org/10.1128/JB.05436-11.
37. Brown JS, Holden DW. Iron acquisition by Gram-positive bacterial pathogens. Microbes Infect. 2002. https://doi.org/10.1016/S1286-4579(02)01640-4.
38. Beasley FC, Marolda CL, Cheung J, Buac S, Heinrichs DE. Staphylococcus *aureus* Transporters Hts, Sir, and Sst Capture Iron Liberated from Human Transferrin by Staphyloferrin A, Staphyloferrin B, and Catecholamine Stress Hormones, Respectively, and Contribute to Virulence. Infect. Immun. 2011. https://doi.org/10.1128/IAI.00117-11
39. Ragsdale SW. (1991). Enzymology of the Acetyl-CoA Pathway of CO2 Fixation. Crit Rev Biochem Mol Biol. 1991. https://doi.org/10.3109/10409239109114070
40. Galushko AS, Schink B. Oxidation of acetate through reactions of the citric acid cycle by *Geobacter sulfurreducens* in pure culture and in syntrophic coculture. Arch Microbiol. 2000. https://doi.org/10.1007/s002030000208.
41. Liu GY, Essex A, Buchanan JT, Datta V, Hoffman HM, Bastian JF, et al. *Staphylococcus aureus* golden pigment impairs neutrophil killing and promotes virulence through its antioxidant activity. J Exp Med. 2005. https://doi.org/10.1084/jem.20050846.
42. Xue L, Chen YY, Yan, Lu W, Wan D, Zhu H. Staphyloxanthin: a potential target for antivirulence therapy. Infect Drug Resist. 2019;12:2151–60. https://doi.org/10.2147/IDR.S193649.
43. Filkins LM, Graber JA, Olson DG, Dolben EL, Lynd LR, Bhuju S, et al. Coculture of Staphylococcus *aureus* with *Pseudomonas aeruginosa* drives S. *Aureus* towards Fermentative Metabolism and reduced viability in a cystic fibrosis model. J Bacteriol. 2015. https://doi.org/10.1128/JB.00059-15.
44. López D, Vlamakis H, Kolter R, Biofilms. Cold Spring Harb Perspect Biol. 2010. https://doi.org/10.1101/cshperspect.a000398.
45. DeLeon S, Clinton A, Fowler H, Everett J, Horswill AR, Rumbaugh KP. Synergistic interactions of *Pseudomonas aeruginosa* and *Staphylococcus aureus* in an in vitro wound model. Infect Immun. 2014. https://doi.org/10.1128/IAI.02198-14.
46. Antikainen J, Kupannen V, Lähteenmäki K, Korhone TK. pH-Dependent Association of Enolase and Glyceraldehyde-3-Phosphate dehydrogenase of *Lactobacillus crispatus* with the cell wall and lipoteichoic acids. J Bacteriol. 2007. https://doi.org/10.1128/JB.00378-07.
47. Ong JS, Taylor TD, Wong CB, Khoo BY, Sasidharan S, Choi SB, et al. Extracellular transglycosylase and glyceraldehyde-3-phosphate dehydrogenase attributed to the anti-staphylococcal activity of *Lactobacillus plantarum* USM8613. J Biotechnol. 2019. https://doi.org/10.1016/j.jbiotec.2019.05.006.
48. Sugimoto S, Iwamoto T, Takada K, Okuda K, Tajima A, Iwase T, et al. *Staphylococcus epidermidis* Esp Degrades Specific Proteins Associated with *Staphylococcus aureus* Biformationmatiohostd Host-Pathogen Interaction. J Bacteriol. 2013. https://doi.org/10.1128/JB.01672-12.
49. Matilla MA, Ortega Á, Krell T. The role of solute binding proteins in signal transduction. Comput Struct Biotechnol J. 2021. https://doi.org/10.1016/j.csbj.2021.03.029.
50. Tuchscherr L, Bischoff M, Lattar SM, Llana MN, Pförtner H, Niemann S, et al. Sigma factor SigB is crucial to mediate *Staphylococcus aureus* Adaptation during Chronic infections. PLOS Pathog. 2015. https://doi.org/10.1371/journal.ppat.1004870.
51. Bischoff M, Dunman P, Kormanec J, Macapagal D, Murphy E, Mounts W, et al. Microarray-based analysis of the *Staphylococcus aureus* σB Regulon. J Bacteriol. 2004. https://doi.org/10.1128/JB.186.13.4085-4099.2004.
52. Junecko JM, Zielinska AK, Mrak LN, Ryan DC, Graham JW, Smeltzer MS, et al. Transcribing virulence in *Staphylococcus aureus*. World J Clin Infect Dis. 2012. https://doi.org/10.5495/wjcid.v2.i4.63.
53. Rachid S, Ohlsen K, Wallner U, Hacker J, Hecker M, Ziebuhr W. Alternative transcription factor ςB is involved in regulation of Biofilm expression in a *Staphylococcus aureus* Mucosal isolate. J Bacteriol. 2000. https://doi.org/10.1128/JB.182.23.6824-6826.2000.
54. Campbell J, Singh AK, Swoboda JG, Gilmore MS, Wilkinson BJ. An antibiotic that inhibits a late step in Wall Teichoic Acid Biosynthesis induces the cell wall stress stimulon in *Staphylococcus aureus*. Antimicrob Agents Chemother. 2012. https://doi.org/10.1128/AAC.05938-11.
55. Weidenmaier C, Peschel A. Teichoic acids and related cell-wall glycopolymers in Gram-positive physiology and host interactions. Nat Rev Microbiol. 2008. https://doi.org/10.1038/nrmicro1861.
56. Xia G, Peschel A. Toward the pathway of *S. Aureus* WTA Biosynthesis. Chem Biol. 2008. https://doi.org/10.1016/j.chembiol.2008.02.005.
57. Xue L, Chen YY, Yan Z, Lu W, Wan D, Zhu H. Staphyloxanthin: a potential target for antivirulence therapy. Infect Drug Resist. 2019. https://doi.org/10.2147/IDR.S193649.
58. Brown JS, Holden DW. Iron acquisition by Gram-positive bacterial pathogens. Microbes Infect. 2002;4:1149–56. https://doi.org/10.1016/S1286-4579(02)01640-4.
59. Johnson M, Sengupta M, Purves J, Tarrant E, Williams PH, Cockayne A, et al. Fur is required for the activation of virulence gene expression through the induction of the sae regulatory system in *Staphylococcus aureus*. Int J Med Microbiol. 2011. https://doi.org/10.1016/j.ijmm.2010.05.003.
60. Litwin CM, Calderwood SB. Role of iron in regulation of virulence genes. Clin Microbiol Rev 1993 https://doi.org/10.1128/CMR.6.2.137
61. Gross M, Cramton SE, Götz F, Peschel A. Key role of Teichoic Acid Net Charge in *Staphylococcus aureus* colonization of Artificial surfaces. Infect Immun. 2001;69:3423–6. https://doi.org/10.1128/IAI.69.5.3423-3426.2001.
62. Ziebandt A-K, Kusch H, Degner M, Jaglitz S, Sibbald MJJB, Arends JP, et al. Proteomics uncovers extreme heterogeneity in the *Staphylococcus aureus* exoproteome due to genomic plasticity and variant gene regulation. Proteomics. 2010;10:1634–44. https://doi.org/10.1002/pmic.200900313.
63. Muthukrishnan G, Quinn GA, Lamers RP, Diaz C, Cole AL, Chen S, et al. Exoproteome of *Staphylococcus aureus* reveals putative determinants of nasal carriage. J Proteome Res. 2011;10:2064–78. https://doi.org/10.1021/pr200029r.
64. Lin MH, Li C, Shu JC, Chu HW, Liu CC, Wu CC. Exoproteome Profiling reveals the involvement of the Foldase PrsA in the cell Surface properties and Pathogenesis of *Staphylococcus aureus*. Proteomics. 2018. https://doi.org/10.1002/pmic.201700195.
65. Zhao X, Palma Medina LM, Stobernack T, Glasner C, de Jong A, Utari P, et al. Exoproteome heterogeneity among closely related Staphylococcus aureus t437 isolates and possible implications for virulence. J Proteome Res. 2019;2019. https://doi.org/10.1021/acs.jproteome.9b00179.
66. Perez-Riverol Y, Bai J, Bandla C, Hewapathirana S, García-Seisdedos D, Kamatchinathan, et al. The PRIDE database resources in 2022: a hub for mass spectrometry-based proteomics evidences. Nucleic Acids Res. 2022. https://doi.org/10.1093/nar/gkab1038.

Publisher's note